Electronic Supplementary Information

Critical Role of {002} Preferred Orientation on Electronic Band Structure of Electrodeposited Monoclinic WO_3 Thin Films

Wai Ling Kwong,[a,b] Pramod Koshy,[a] Judy N. Hart,[a] Wanqiang Xu,[a] and Charles C. Sorrell [a]*

[a] School of Materials Science and Engineering, UNSW Sydney, NSW 2052, Australia

[b] Department of Chemistry-Ångström Laboratory, Molecular Biomimetics, Uppsala University, S-75120 Uppsala, Sweden

*Corresponding author: C.Sorrell@unsw.edu.au; Tel. (+61-2) 9385-4421; Fax. (+61-2) 9385-6565

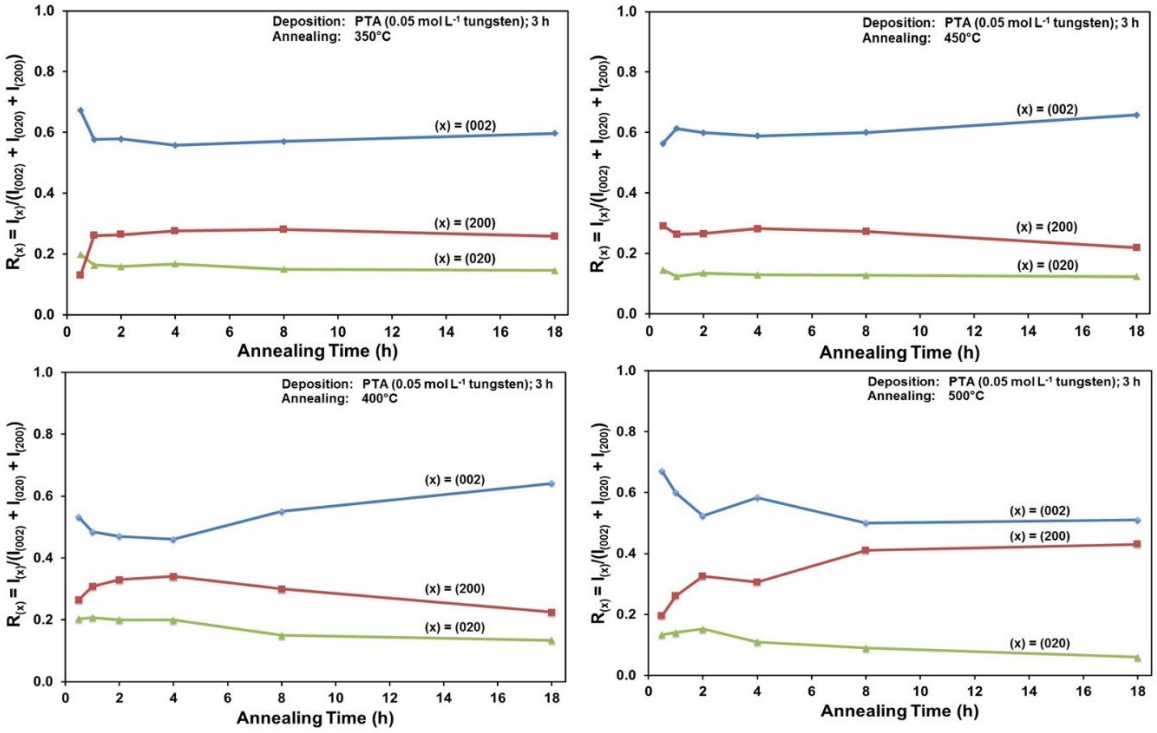

Figure S1. Relative XRD intensities $R_{(x)} = I_{(x)}/(I_{(002)} + I_{(020)} + I_{(200)})$ (where (x) = (002), (020), or (200)) as a function of annealing time for the films deposited from PTA consisting of 0.05 mol L^{-1} tungsten and annealed at fixed temperatures in the range 350º-500ºC.

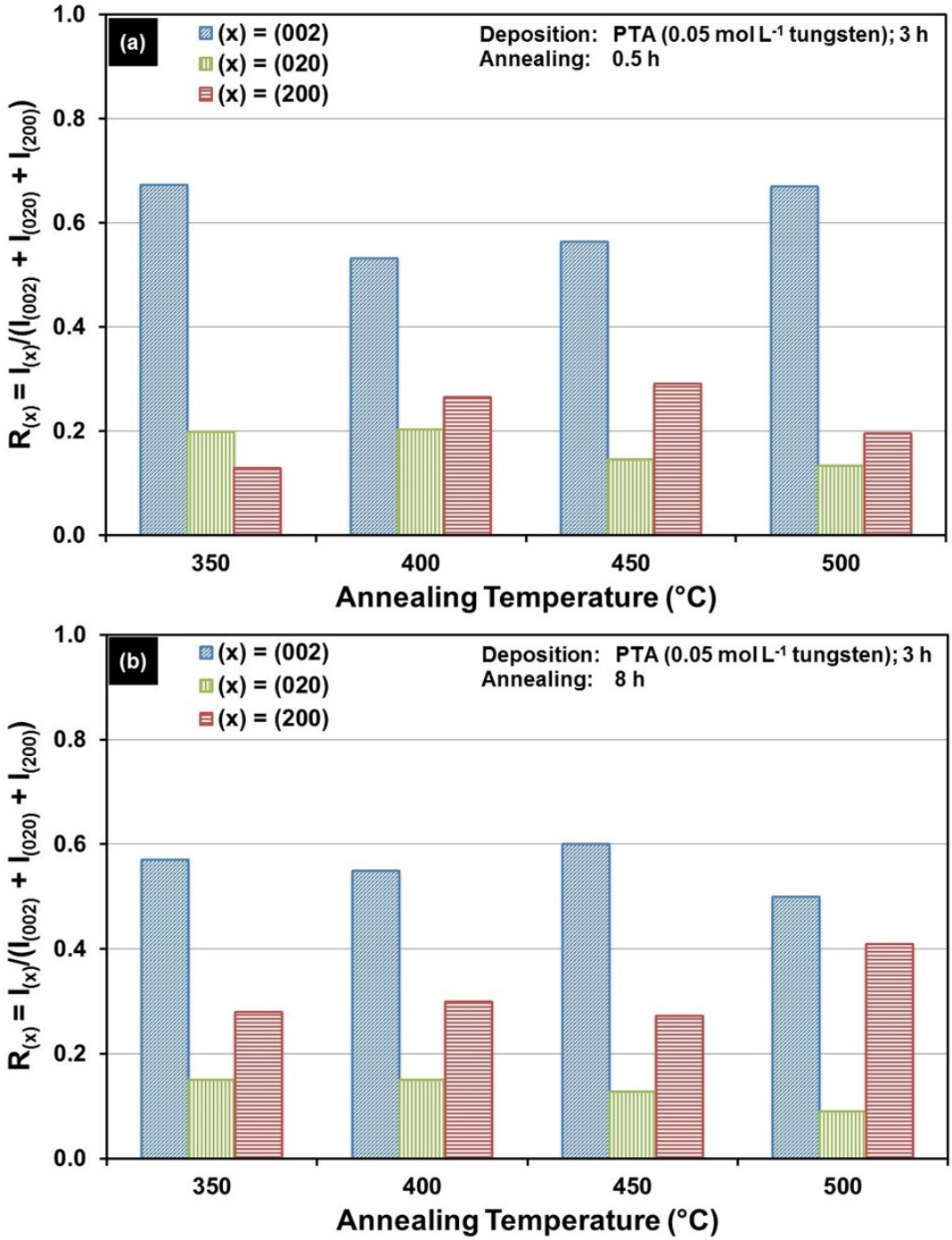

Figure S2. Relative XRD intensities $R_{(x)} = (I_{(x)}/(I_{(002)} + I_{(020)} + I_{(200)})$ (where (x) = (002), (020), or (200)) as a function of annealing temperature for the films deposited from PTA consisting of 0.05 mol L^{-1} tungsten and annealed for (a) 0.5 h or (b) 8 h.

Film	(002)	(020)	(200)
$\mathbf{T_{(002)}}$	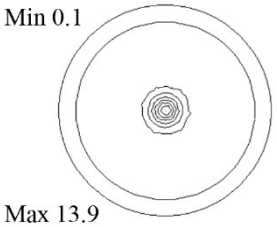	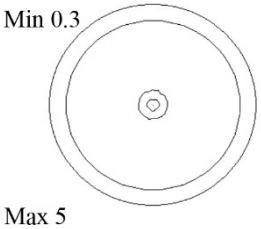	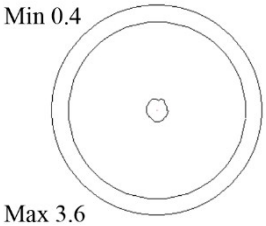
$\mathbf{T_{(002) + (200)}}$	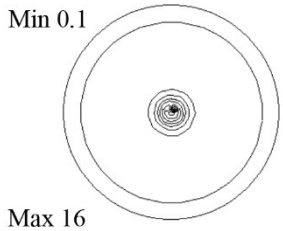	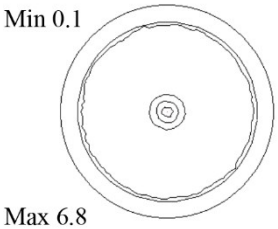	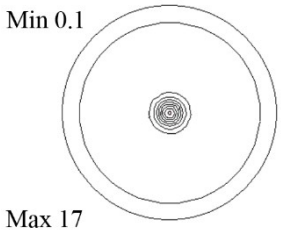
$\mathbf{T_{(200)}}$	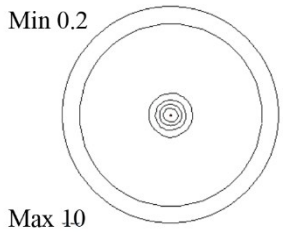	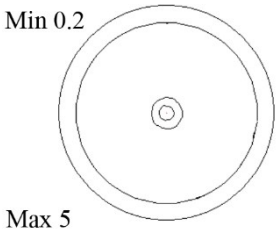	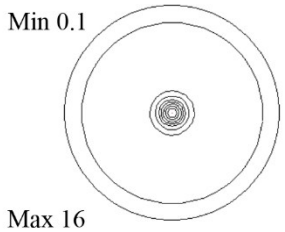

Figure S3. Pole figure measurements for the {002} planes of the films. Contours of normalised linear distribution densities (2, 4, 6, …) are shown with the maximal and minimal densities indicated on the left of each pole figure.

(i) *Film $T_{(002)}$*:
A dominant (002) texture is formed where the orientation density concentrated at the centre of the pole is 13.9, which is much higher than 5 and 3.6 for (020) and (200) textures, respectively, implying that the (002) plane in the majority of the grains is aligned parallel to the substrate.

(ii) *Film $T_{(002) + (200)}$*:
Two major (002) and (200) and one minor (020) textures are formed where the (002), (200), and (020) components show orientation densities of 15.0, 16.9, and 6.8, respectively. The circumpunct pattern of the pole figure for (020) denotes the co-existence of (020) planes in both parallel and perpendicular alignments with respect to the substrate plane.

(iii) *Film $T_{(200)}$*:
The orientation distribution density at the centre of the pole is 16 for (200) texture, which is higher than 10 and 5 for (002) and (020), respectively, showing that the (200) plane is the dominant plane aligned parallel to the substrate.

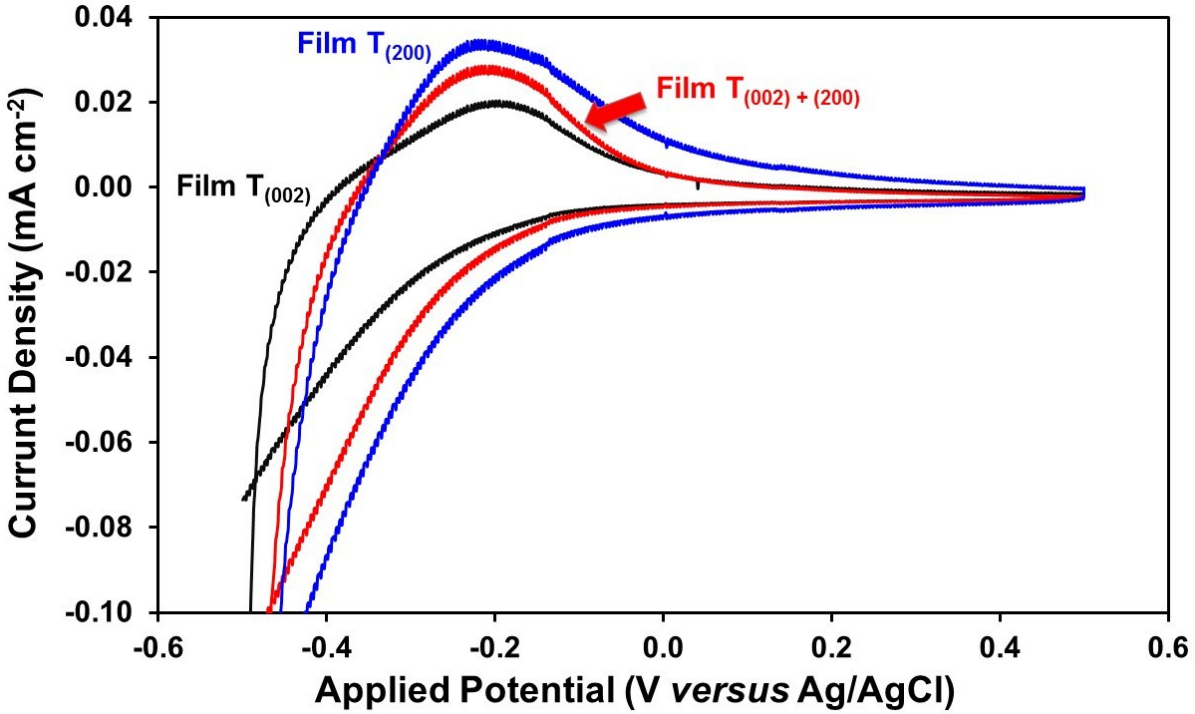

Figure S4. Cyclic voltammograms of films $T_{(002)}$, $T_{(002)+(200)}$, and $T_{(200)}$ measured in 0.5 mol L^{-1} NaCl aqueous solution in dark environment.

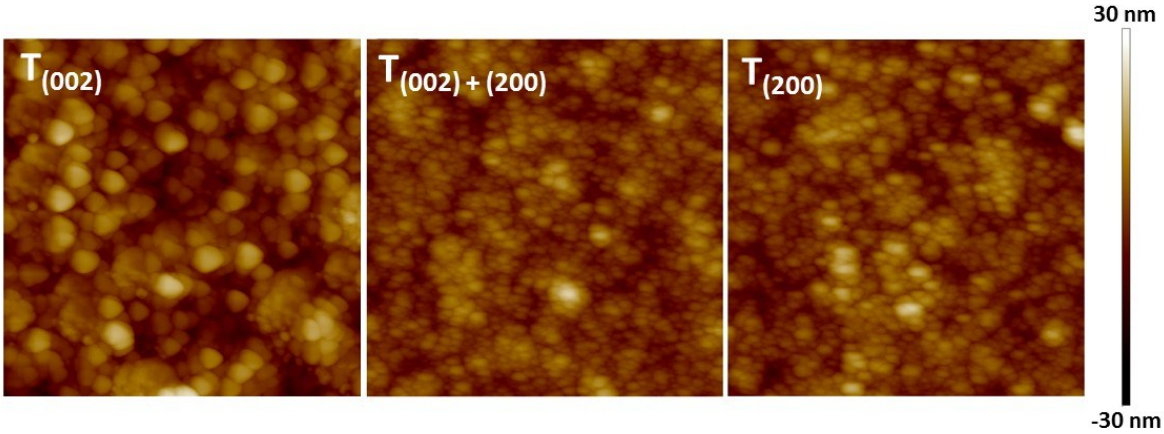

Figure S5. AFM images (scanned area: 3 μm × 3 μm) of films $T_{(002)}$, $T_{(002)+(200)}$, and $T_{(200)}$. The surface area ratios (3D surface area/2D projected surface area), analysed using Bruker NanoScope Analysis v1.4 software, were very similar (1.0085 ± 0.0006) and so are unlikely to be a factor contributing to the differences in the photoelectrochemical and photocatalytic performances.

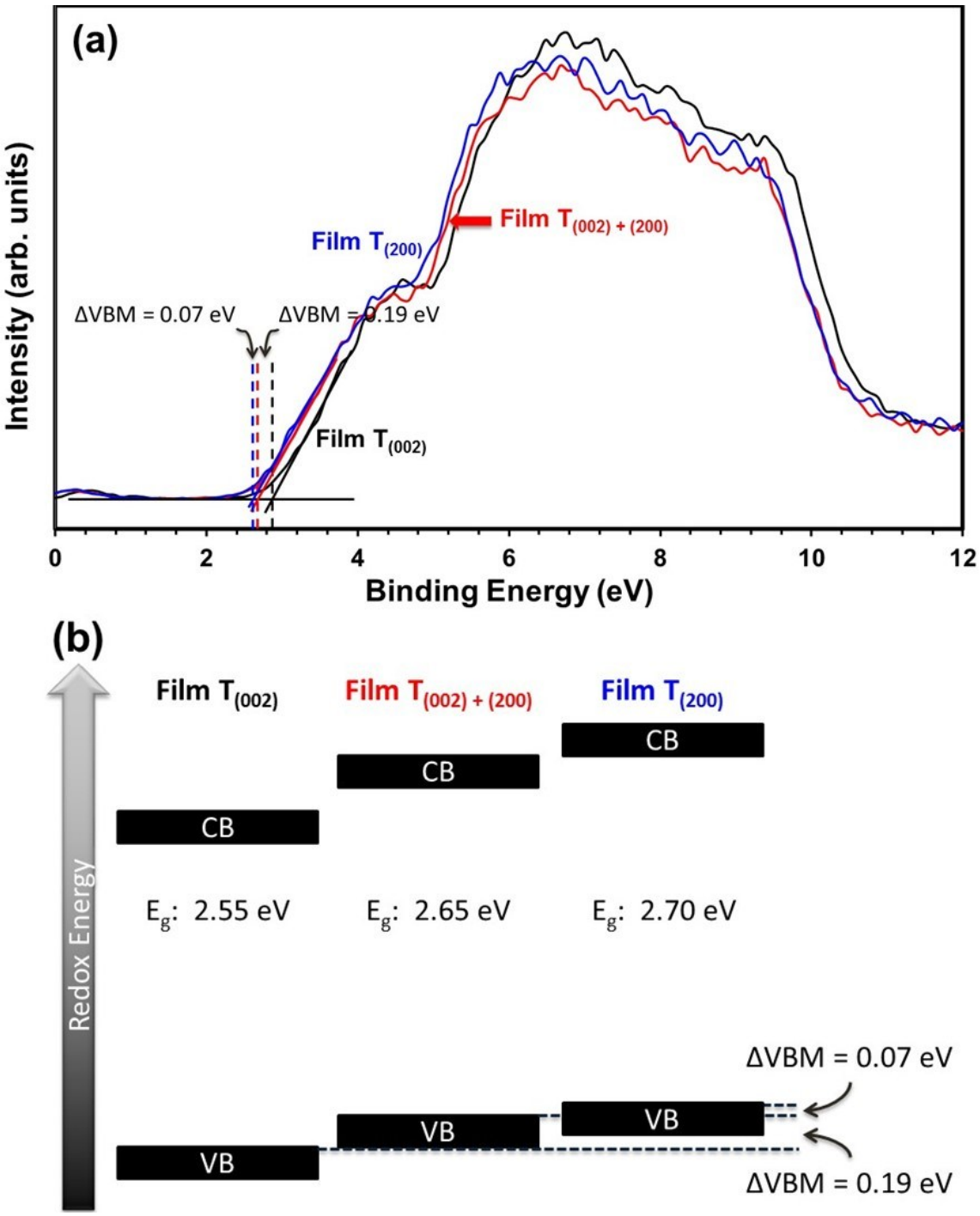

Figure S6. (a) XPS valence band and (b) electronic band structure of films $T_{(002)}$, $T_{(002)+(200)}$, and $T_{(200)}$ determined using XPS (**Figure** S6(a)) and UV-Visible spectrophotometry (**Figure** 7); E_g, CB, VB, and ΔVBM are optical indirect band gap, conduction band, valence band, and energy difference in valence band maxima, respectively.

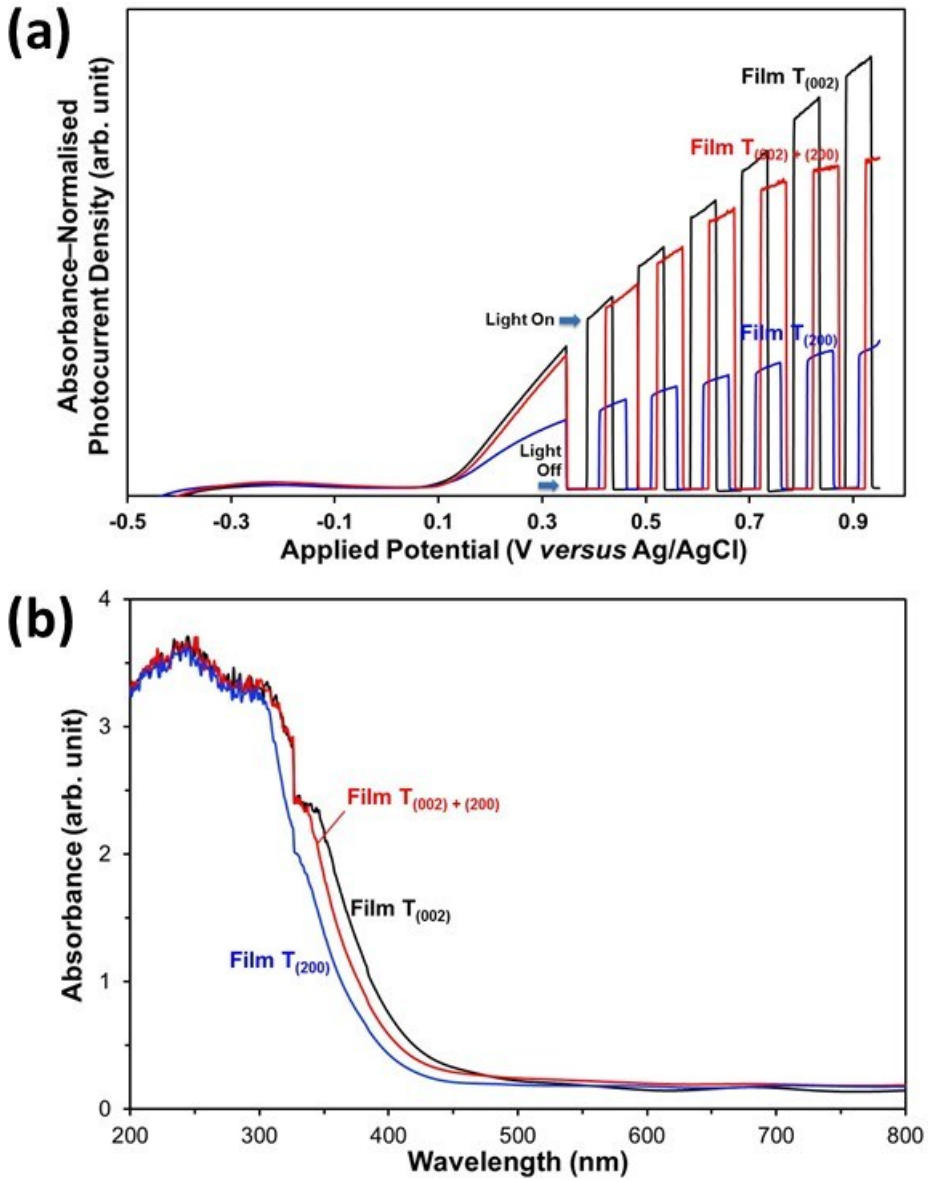

Figure S7. (a) Photocurrent densities normalised to the total optical absorbances of films $T_{(002)}$, $T_{(002)+(200)}$, and $T_{(200)}$; the total optical absorbances were obtained by calculating the area under the optical absorbance-wavelength curves shown in **Figure** S7 (b).

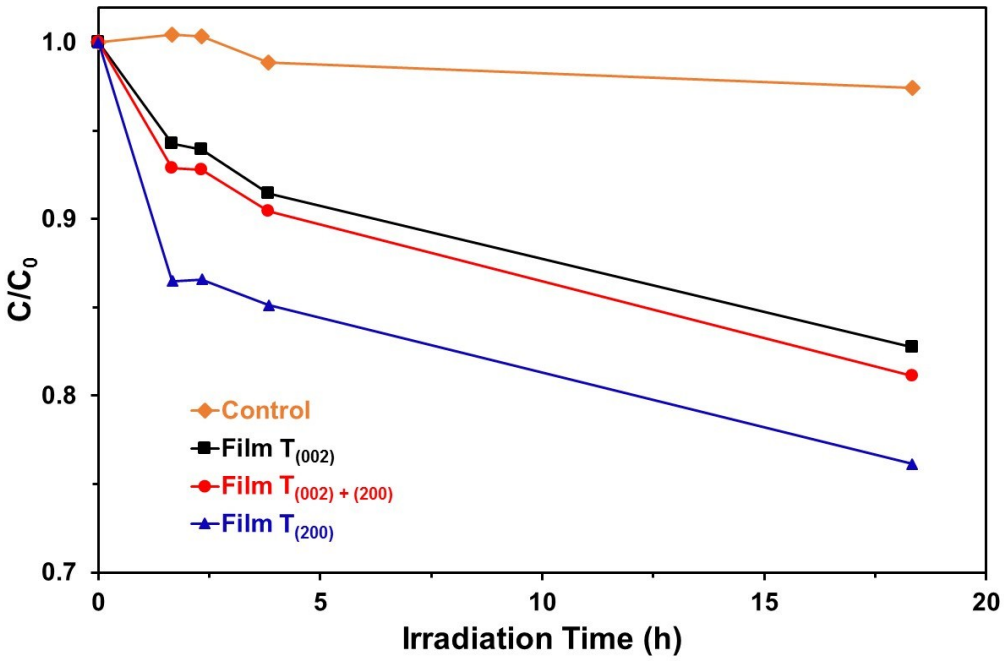

Figure S8. Photocatalytic degradation of methylene blue as a function of irradiation time *t*; C and C_0 are the concentrations of methylene blue at irradiation time *t* and *t* = 0, respectively; major spectral output: 365 nm; C_0 = 4.5 ppm.